Mobility of TrkA Is Regulated by Phosphorylation and Interactions with the Low-Affinity NGF Receptor†

David E. Wolf,*,‡ Christine McKinnon-Thompson,‡ Marie-Claire Daou,‡ Robert M. Stephens,§ David R. Kaplan,|| and Alonzo H. Ross‡

Departments of Physiology and Pharmacology, University of Massachusetts Medical School, 55 Lake Avenue North, Worcester, Massachusetts 01655, ABL-Basic Research Program, National Cancer Institute, Frederick Cancer Research and Development Center, Frederick, Maryland 21701, and Montreal Neurological Institute, Montreal, Quebec H3A 2B4, Canada

Received August 5, 1997; Revised Manuscript Received November 25, 1997

ABSTRACT: The nerve growth factor (NGF) receptor is a complex of two proteins, gp75 and the tyrosine kinase TrkA. Using fluorescence recovery after photobleaching, we have studied the diffusion properties of the TrkA receptor. For PC12 cells that express both gp75 and TrkA, TrkA was relatively immobile with only 28 ± 1% of receptor molecules free to diffuse with $D = (3.64 \pm 0.23) \times 10^{-9}$ cm^2/s. Addition of NGF decreased the mobile fraction to 21 ± 1% with $D = (4.11 \pm 0.18) \times 10^{-9}$ cm^2/s. Using the Sf9 baculovirus expression system, we were able to study TrkA in the absence and presence of gp75. On Sf9 cells, TrkA showed a mobile fraction of 46 ± 2% with $D = (2.64 \pm 0.21) \times 10^{-9}$ cm^2/s in the absence of gp75 and 43 ± 2% with $D = (2.31 \pm 0.25) \times 10^{-9}$ cm^2/s in its presence. Thus, gp75 did not alter TrkA mobility. Addition of NGF to the medium approximately halved the mobile fraction for TrkA in both the absence and presence of gp75. However, using a kinase-deficient mutant of TrkA, we found that ligand-induced immobilization requires an active kinase in the absence of gp75 but not in its presence. In addition, using point mutations at specific TrkA autophosphorylation sites, we determined that mobility is controlled by multiple phosphorylation sites, but the SHC binding site at Y490 may be particularly important for ligand-induced immobilization of TrkA. Therefore, two mechanisms lead to NGF-induced immobilization of TrkA—the first resulting from autophosphorylation of TrkA and the second occurring through TrkA's association with gp75.

Ligand-induced immobilization of receptor tyrosine kinases during receptor-mediated activation was originally described for the nerve growth factor (NGF)[1] (*1*), epidermal growth factor (*2*, *3*), and insulin receptors (*2*, *3*). For each of these receptors, binding of the corresponding growth factor induced tyrosine activation and immobilization of the receptor. Although there was considerable evidence for this phenomenon, the mechanism of immobilization was unknown. It was not clear whether immobilization resulted from receptor aggregation, phosphorylation, or association with other membrane components. In recent years, our understanding of receptor activation and signal tranduction has grown immensely, but the topic of ligand-induced immobilization of receptors has remained a mystery. In this paper we examine immobilization of nerve growth factor receptor TrkA in relation to ligand binding, homo- and heterodimerization, and receptor phosphorylation.

NGF is an essential factor required for the development, maintenance, and repair of the nervous system (*4*). All of the actions of NGF are thought to result from the action of two cell surface receptors, gp75 and TrkA (*5*, *6*). Gp75 is a 75 000-Da glycoprotein with a cysteine-rich extracellular domain, a single transmembrane domain, and a 155-amino acid cytoplasmic domain (*7*, *8*). There is evidence that gp75 can activate signal transduction through cytoplasmic kinases (*9*, *10*), sphingomyelin hydrolysis (*11*), and transcription factor NF-κB (*12*, *13*). The second NGF receptor is TrkA, a 140 000-Da glycoprotein with a single transmembrane domain and a 304-amino acid cytoplasmic domain that contains a tyrosine kinase domain (*6*). NGF activates TrkA autophosphorylation but does not result in tyrosine phosphorylation of gp75 (*14*, *15*). Tyrosine autophosphorylation sites on TrkA include the following: the SHC binding domain at Y490, the phospholipase Cγ1 (PLCγ1) binding domain at Y785, and three sites within the kinase domain Y670, Y674, and Y675 that regulate phosphorylation activity (*16*, *17*).

A number of experiments indicate that the two NGF receptors interact and synergize with each other. Transgenic mice that lack gp75 have neurological deficiencies involving the death of TrkA-positive sensory neurons (*18*). Both gp75

† This work was supported in part by National Institutes of Health Grants NS28760 (to D.E.W. and A.H.R.) and NS21716 (A.H.R.).

* To whom all correspondence should be addressed: Department of Physiology, University of Massachusetts Medical School, 55 Lake Avenue North, Worcester, MA 01655. (tel) 508-842-8921; (fax) 508-842-9632; (e-mail) Wolf@Sci.Wfbr.edu.

‡ University of Massachusetts Medical School.

§ National Cancer Institute.

|| Montreal Neurological Institute.

[1] Abbreviations: NGF, nerve growth factor; BDNF, brain-derived neurotrophic factor; *D*, diffusion coefficient; DMEM, Dulbecco's Minimum Essential Medium; FRAP, fluorescence recovery after photobleaching; mAb, monoclonal antibody; moi, multiplicity of infection; na, numerical aperature; PLCγ1, phospholipase Cγ1; PKC, protein kinase C; *R*, recovery (in percent).

S0006-2960(97)01925-9 CCC: $15.00
Published on Web 02/12/1998

and TrkA undergo retrograde transport from the synapse to the cell body (*19*−*21*). In cell culture models, coexpression of gp75 enhances the biological response of cells expressing TrkA (*22*−*26*). Although Jing et al. (*27*) reported that TrkA is sufficient for high-affinity NGF binding, Hempstead et al. (*28*) found that expression of both gp75 and TrkA is required for high-affinity binding. In addition, coexpression of gp75 with TrkA enhances the rate of NGF binding (*29*). The antibody to gp75 inhibits responses of PC12 cells to NGF (*30, 31*). TrkA is essential for NGF activation of protein kinases associated with the cytoplasmic domain of gp75 (*9, 10*). The synergistic action of these receptors has led to the hypothesis that gp75 and TrkA form a heteromolecular complex which is the high-affinity NGF receptor (*28*).

Using fluorescence recovery after photobleaching (FRAP), we have shown that gp75 in coexpressing cells is immobilized through interactions with TrkA (*32*). This immobilization, like high-affinity binding (*28*), does not occur for gp75(Xba), a mutant form of gp75 lacking most of its intracellular domain (*22*). NGF causes some immobilization of gp75 probably due to cross-linking between receptors by dimeric NGF in either the absence or presence of TrkA (*32*). In addition, NGF increases the diffusion rate of gp75 and gp75(Xba) in the presence of TrkA. These results suggest that the requirements for gp75−TrkA complex formation are different from those for immobilization. Extracellular and/or transmembrane domains of gp75 and TrkA are critical for interaction and complex formation. However, receptor immobilization requires, in addition, intact intracellular domains.

By a copatching assay, we have demonstrated that gp75 and TrkA interact with one another to form a heteromolecular complex. In contrast, gp75 does not complex with the brain-derived neurotrophic factor receptor, TrkB, the platelet-derived growth factor, PDGF, receptor, or the *Drosophila* receptor, Torso (*33*). Complexing does not require the kinase activity of TrkA. Using chimeric TrkA receptors (*33*), we have shown that complexing between gp75 and TrkA is most influenced by the extracellular domains.

This paper focuses on the mechanism by which NGF leads to immobilization of TrkA. We show that NGF binding to TrkA leads to receptor immobilization by a kinase-dependent mechanism. TrkA receptors modified at individual autophosphorylation sites show altered states of immobilization, indicating that autophosphorylation modulates lateral mobility of TrkA. For cells coexpressing gp75 and TrkA, NGF also leads to immobilization of TrkA, but autophosphorylation of TrkA is not required. These data suggest two underlying causes for receptor immobilization. The first is dependent on autophosphorylation and may involve binding of SH2 domain proteins to autophosphorylation sites (*34*). The second is independent of autophosphorylation and likely involves NGF binding simultaneously to two gp75 molecules, perhaps analogous to the ligand−receptor complex for tumor necrosis factor (*35*). Such bridges between gp75 molecules would lead to clustering and immobilization of the gp75−TrkA complexes. We propose that gp75 stabilizes and promotes the ability of NGF to cross-link and immobilize TrkA. This immobilization may restrict TrkA to signaling complexes or sites within the membrane and thereby spatially restrict autophosphorylation and signal transduction.

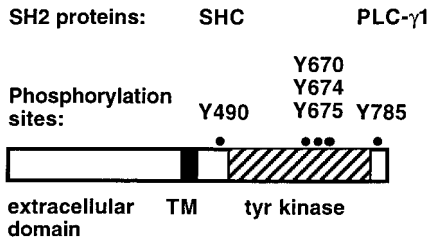

FIGURE 1: Schematic of TrkA, indicating tyrosine phosphorylation sites: the SHC binding site at Y490, sites within the tyrosine kinase domain at Y670, Y674, and Y675, and the PLCγ1 site at Y785.

EXPERIMENTAL PROCEDURES

Antibodies and Fragments. Rabbit anti-TrkA serum RTA (*36*) was generously supplied by Dr. Louis Reichardt (UCSF School of Medicine, San Francisco). IgG was purified from this antiserum on a Bio-Rad protein A column modified to increase the yield by using 100 mM Tris, pH 8.0, as the binding buffer, 10 mM Tris, pH 8.0, as the wash and 100 mM glycine, pH 3.0, as the eluting buffer.

Fab fragments of these mAb's were prepared as previously described (*37, 38*). A fluorescein Fab fragment of goat anti-rabbit IgG was obtained from Cappel (Durham, NC). Rabbit antiserum 203 against the Trk C-terminus (*39*) was used for immunoblotting TrkA. Recombinant anti-phosphotyrosine−horseradish peroxidase conjugate (RC20) was obtained from Transduction Laboratories (Lexington, KY) and used for immunoblotting.

Baculoviruses. Recombinant baculoviruses for human wild-type gp75 and mutant human TrkA were prepared as described previously (*32, 33, 40*).

The structure of TrkA is shown in Figure 1, indicating the major regions: extracellular, transmembrane, and cytoplasmic domains. Also indicated are the sites of tyrosine phosphorylation. Mutations used in this study are TrkA (K538N), a point mutation at the ATP binding site of the kinase domain, TrkA (Y490F), which does not contain the SHC phosphorylation site, TrkA (Y785F), which lacks a PLCγ1 site, TrkA (YY/490,785/FF), which lacks both of these sites, and TrkA (YYY/670,674,675/FFF), which is a triple-point mutation in the regulatory region of the kinase domain, which is kinase-deficient (*16, 17*) like TrkA (K538N).

Cell Lines. Rat pheochromocytoma PC12 cells were maintained in DMEM supplemented by 10% heat-inactivated horse serum, 5% heat-inactivated fetal bovine serum, and 100 μg/mL gentamicin at 37 °C under 5% CO_2 humidified atmosphere. Sf9 insect cells were maintained in TMN−FH medium from JRH Biosciences (Lenexa, KS) supplemented with 10% heat-inactivated fetal bovine serum and 100 mg/mL gentamicin at 28−29 °C.

Baculovirus Expression in Sf9 Cells. To express a single NGF receptor, recombinant baculovirus was added to Sf9 cells (2×10^6 cells in a 25-cm^2 flask) at a multiplicity of infection (moi) of 1 for the gp75 virus or a moi of ~10 for TrkA. For coexpression experiments, TrkA baculovirus was added to Sf9 cells at a moi of ~10 followed by immediate addition of gp75 baculovirus at moi of 1. These conditions resulted in infected cells displaying high-affinity binding of NGF and a ratio of gp75/TrkA proteins similar to that observed for Trk-PC12 cells which are highly responsive to NGF (*32, 39*).

Table 1: Diffusion Data for TrkA on PC12 and Sf9 Cells[a]

NGF receptors	cell	R (%)	SD (% R)	$D \times 10^9$ s/cm^2	SD $\times 10^9$ s/cm^2	n
gp75 + TrkA	PC12	28 ± 1	10	3.64 ± 0.23	2.26	99
gp75 + TrkA + NGF	PC12	21 ± 1	9	4.11 ± 0.18	1.87	106
Gp75 + K538N	Sf9	43 ± 2	18	3.81 ± 0.36	5.42	206
Gp75 + K538N + NGF	Sf9	25 ± 1	7	1.64 ± 0.38	1.19	190
Gp75 + TrkA	Sf9	43 ± 2	22	2.31 ± 0.25	3.99	256
Gp75 + TrkA + NGF	Sf9	29 ± 0.7	10	2.17 ± 0.29	3.44	130
K538N	Sf9	34 ± 1	16	2.72 ± 0.47	5.90	162
K538N + NGF	Sf9	36 ± 1	14	2.27 ± 0.25	2.83	133
YYY/670,674,675/FFF	Sf9	32 ± 1	18	2.89 ± 0.25	2.94	112
YYY/670,674,675/FFF + NGF	Sf9	35 ± 2	20	2.62 ± 0.24	2.55	116
TrkA	Sf9	46 ± 2	21	2.64 ± 0.21	3.16	233
TrkA + NGF	Sf9	23 ± 1	7	1.73 ± 0.11	1.27	148
YY/490,785/FF	Sf9	30 ± 1	16	2.59 ± 0.23	2.74	148
YY/490,785/FF + NGF	Sf9	33 ± 1	15	3.04 ± 0.39	3.74	98
Y490F	Sf9	47 ± 2	17	1.95 ± 0.14	1.54	120
Y490F + NGF	Sf9	48 ± 2	19	2.66 ± 0.20	2.09	107
Y785F	Sf9	38 ± 1	16	2.03 ± 0.16	1.39	125
Y785F + NGF	Sf9	33 ± 1	13	2.59 ± 0.19	1.98	114

[a] D and R given as mean ± standard error of the mean. SD, standard deviation; n, number of single bleach measurements.

Measurement of TrkA Autophosphorylation. Cells (6×10^6/sample) were treated for 10 min with 4 nM NGF in complete medium. The cells were extracted at 4 °C with 0.5% (v/v) NP-40, 140 mM NaC1, 10 mM Tris, 10 mM NaF, 5 mM Na_2EDTA, 100 kallikrein IU/mL of aprotinin, 10 mM Na_2VO_4, and 1 mM phenylmethanesulfonyl fluoride, pH 7.5, and then clarified by centrifugation at 76000*g* for 1 h. TrkA was immunoprecipitated with 203 anti-Trk C-terminus rabbit serum (1:500) (*39*) and applied to a 10% SDS polyacrylamide gel. After electrophoresis, the proteins were electrotransferred to an Immobilon-P membrane (Millipore, Bedford, MA), followed by blocking for 1 h at 37 °C with 1% BSA (w/v), 0.1% Tween-20 (v/v), 137 mM NaCl, 20 mM Trizma, pH 7.6. The membrane was then incubated for 1 h at 37 °C with an RC20 anti-phosphotyrosine antibody−horseradish peroxidase conjugate (0.2 mg/mL) (Transduction Laboratories). Reactive bands were visualized with a chemiluminescent substrate (*41*). The membrane was then stripped by a 45-min incubation at 70 °C in 2% SDS (w/v), 100 mM β-mercaptoethanol, 62.5 mM Trizma, pH 6.8. The membrane was then probed with 203 anti-Trk antiserum, washed, and incubated with horseradish peroxidase-conjugated goat anti-rabbit IgG secondary antibody (1:1000) (Amersham, Arlington Heights, IL) and finally with chemiluminescent substrate.

Labeling of Cells for FRAP Measurements. For FRAP measurements, PC12 cells (5×10^5) were incubated for 30 min at room temperature with 50 μL of an anti-TrkA Fab fragment of rabbit antibody RTA (0.1 mg/mL in Dulbecco's Minimum Essential Medium (DMEM) supplemented with 1% fetal bovine serum and 20 mM HEPES, pH 7.4). The samples were centrifuged, and the cells were washed twice with 200 μL of medium. The cells then were incubated for 30 min with 25 μg/mL fluorescein Fab fragment of anti-rabbit IgG. The cells were then pelleted through a cushion of DMEM with 5% fetal bovine serum. Since serum lacks detectable NGF, the serum present in these washes does not obscure the effects of added NGF (*42*).

FRAP measurements on Sf9 cells were carried out ~60 h postinfection. Cells (2.5×10^5) were incubated for 30 min at room temperature with 25 μL of a Fab fragment of RTA antibody in Sf9 growth medium (0.1 mg/mL). The samples were washed by centrifugation (53*g*) for 3 min. The cells were suspended in 25 μg/mL fluorescein Fab fragment of anti-rabbit IgG and incubated for 20 min at room temperature. The cells were washed by centrifugation and then were pelleted through a cushion of TMN−FH medium with 10% fetal bovine serum. FRAP measurements were performed as previously described (*37, 38*). For measurements made in the presence of NGF, the cells were resuspended in medium containing 4 nM of NGF immediately prior to measurements. For both PC12 and Sf9 cells, all measurements were made at room temperature within 30 min of labeling, during which time no detectable internalization was observed.

FRAP Measurements. The specific designs of our FRAP instrument and data analysis algorithm have been described in detail (*43*). All FRAP measurements were made as described previously (*37, 38*) at room temperature using a Leitz 63× na 1.4 planapochromat objective and the 488-nm line of a Lexel 95−2 argon laser. At the object plane of the microscope, the laser beam in this system has the form

$$I(x,y) = I_o \exp(-2(x^2 + y^2)/w^2)$$

where I_o is the intensity at the center, x and y are the Cartesian coordinates in the plane of the object, and w is the beam radius, 0.9 μm. The monitoring intensity was 0.13 μW, and the bleaching intensity was 1.3 mW for 25 ms. These conditions were chosen so that there would be no significant bleaching due to the monitoring beam. Samples were discarded if solution background intensities exceeded 10%. Data were fitted to the diffusion theory of Axelrod et al. (*44*) by a modification of the nonlinear least-squares procedure of Bevington (*43, 45, 46*). FRAP data are presented as averages (±SEM) of n single bleach measurements made on n separate cells. Additionally, the standard deviations are given in Table 1 as a measure of the widths of the distributions.

Typical FRAP recovery curves are shown in Figure 2 for TrkA expressed in Sf9 cells in the absence and presence of NGF. If $F(t < 0)$ is the prebleach fluorescence intensity, $F(0)$ the fluorescence intensity immediately following the bleach, and F(∞) the fluorescence intensity after recovery is

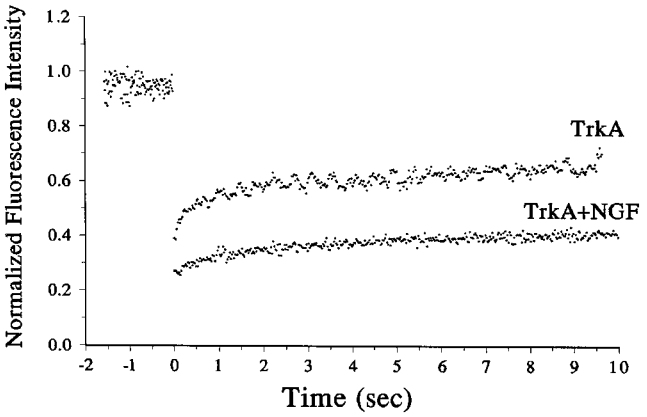

FIGURE 2: Typical FRAP recovery curves showing the diffusion of TrkA expressed in Sf9 insect cells in the absence or presence of NGF. Data have been normalized by dividing by the average prebleach intensity so that $F(t<0) = 1.0$. Each cell was bleached for ~25 ms. The $R = 46\%$ and 23% in the absence and presence of NGF, respectively. The corresponding diffusion coefficients are $D = 2.64 \times 10^{-9}$ cm^2/s and $D = 1.70 \times 10^{-9}$ cm^2/s.

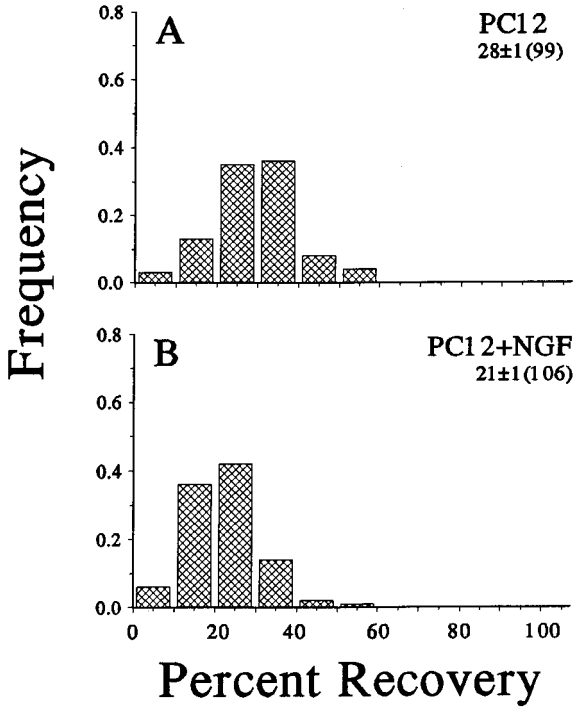

FIGURE 3: Histograms showing frequency of mobile fractions for diffusion of TrkA expressed in PC12 cells. Means, standard errors, standard deviations, and numbers of measurements are also given in Table 1 for both R and D. Panel A shows data for untreated PC12 cells ($R = 28 \pm 1\%$, (mean ± SEM), $n = 99$), B shows data for PC12 cells treated with NGF ($R = 21 \pm 1\%$, $n = 106$).

complete, then the percent $R = (F(\infty) - F(0))/(F(t < 0) - F(0))$. Diffusion coefficients are calculated by fitting the recovery curves to the diffusion equation by nonlinear least squares. The specifics of our algorithm have been described (*43*).

RESULTS

NGF-Induced Immobilization of TrkA on Mammalian Cells. FRAP measurements of TrkA diffusion on mammalian PC12 cells are summarized in Table 1 and Figures 3 and 4. TrkA shows diffusion properties typical of membrane spanning proteins, with $D = (3.64 \pm 0.23) \times 10^{-9}$ cm^2/s and $R = 28 \pm 1\%$. The diffusive properties of TrkA are similar to those already reported for gp75 diffusion (*32*) on the same cells. Following addition of 4 nM NGF, we obtained $D = (4.11 \pm 0.18) \times 10^{-9}$ cm^2/s and $R = 21 \pm 1\%$. Thus, NGF caused a reduction of R ($p \leq 0.0005$, Student t-test) but no significant change in the diffusion coefficient. Additionally F-tests do not indicate significant changes in the width of distributions for either D or R.

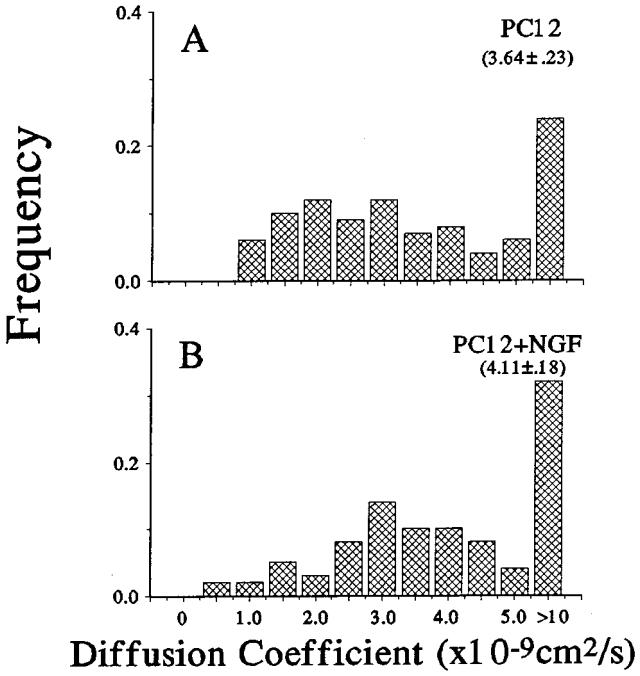

FIGURE 4: Histograms showing frequency of diffusion coefficients for diffusion of TrkA expressed in PC12 cells. Panel A shows data for untreated PC12 cells ($D = (3.64 \pm 0.23) \times 10^{-9}$ cm^2/s, $n = 98$). B shows data for PC12 cells treated with NGF ($D = (4.11 \pm 0.18) \times 10^{-9}$ cm^2/s, $n = 103$).

TrkA Diffusion on Sf9 Cells. To further study NGF-induced immobilization of TrkA, we employed the baculovirus−insect cell expression system which was useful for similar studies of gp75 diffusion (*32*) (Table 1 and Figures 5 and 6).

We have previously shown that in the native state TrkA and gp75 complex together as subunits to form the functional high-affinity nerve growth factor receptor on Sf9 cells (*32*, *33*). Thus, the condition of TrkA coexpressed with gp75 on Sf9 cells mimics the state of the TrkA receptor on mammalian cells such as PC12. It should be noted that under the conditions used in our experiments the gp75 and TrkA are expressed approximately stoichiometrically (*32*). We found that TrkA diffused with $D = (2.31 \pm 0.25) \times 10^{-9}$ cm^2/s and $R = 43 \pm 2\%$. As we found for PC12 cells treatment of (gp75+TrkA)-expressing Sf9 cells with NGF led to immobilization of TrkA $R = 29 \pm 1\%$ ($p \leq 0.0005$, Student t-test). In addition, treatment with NGF decreased the width of the distribution (F-test, $p \leq 0.01$). There was no significant effect of NGF on the average diffusion coefficient, $D = (2.17 \pm 0.29) \times 10^{-9}$ cm^2/s but there was a narrowing of the distribution of D (F-test, $p \leq 0.01$).

The Sf9 cell system also allows us to use mutant forms of the receptors. We tested the effect of coexpression of gp75 with TrkA (K538N), which has a point mutation at the ATP binding site that abolishes kinase activity and

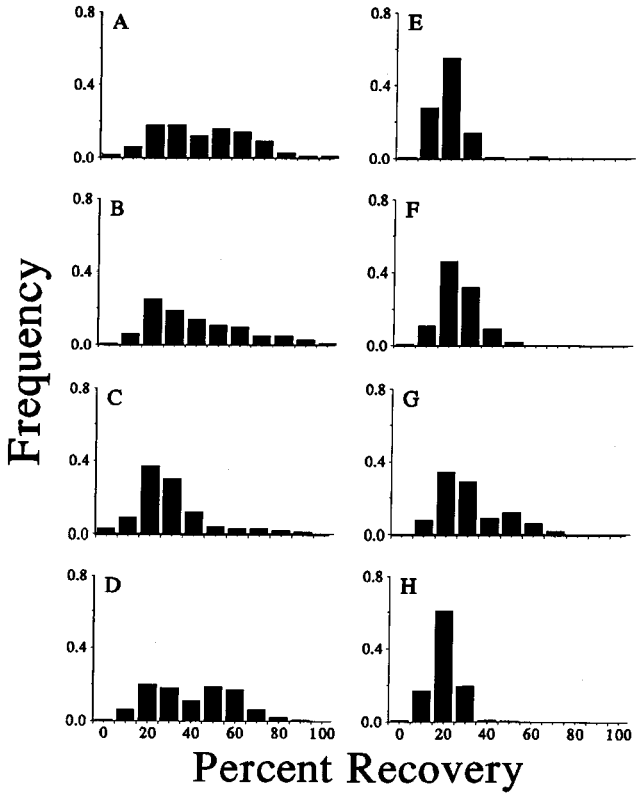

FIGURE 5: Histograms showing frequency of mobile fractions for diffusion of TrkA expressed in Sf9 insect cells. Means, standard errors, standard deviations, and numbers of measurements are given in Table 1 for both *R* and *D*. (A) TrkA expressed alone ($n = 233$); (B) gp75 coexpressed with TrkA ($n = 256$); (C) TrkA(K538N) expressed alone ($n = 162$); (D) gp75 coexpressed with TrkA-(K538N) ($n = 206$); (E) TrkA expressed alone + NGF ($n = 148$); (F) gp75 coexpressed with TrkA + NGF ($n = 130$); (G) TrkA (K538N) expressed alone + NGF ($n = 133$); (H) gp75 coexpressed with TrkA (K538N) + NGF ($n = 190$).

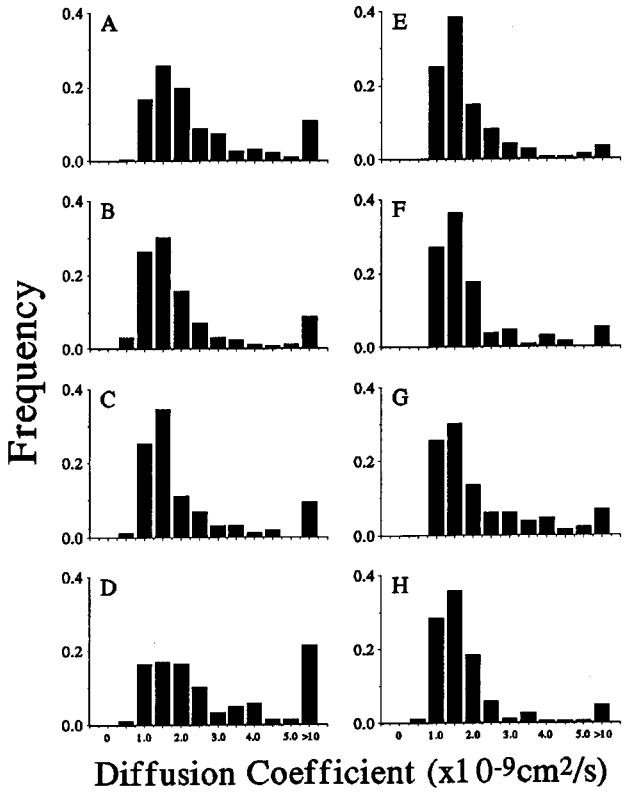

FIGURE 6: Histograms showing frequency of diffusion coefficients for diffusion of TrkA expressed in Sf9 insect cells. Means, standard errors, standard deviations, and numbers of measurements are given in Table 1 for both *R* and *D*. (A) TrkA expressed alone ($n = 233$); (B) gp75 coexpressed with TrkA ($n = 256$); (C) TrkA (K538N) expressed alone ($n = 162$); (D) gp75 coexpressed with TrkA (K538N) ($n = 206$); (E) TrkA expressed alone + NGF ($n = 148$); (F) gp75 coexpressed with TrkA + NGF ($n = 130$); (G) TrkA (K538N) expressed alone + NGF ($n = 133$); (H) gp75 coexpressed with TrkA (K538N) + NGF ($n = 190$).

autophosphorylation. For TrkA (K538N) coexpressed with gp75, we found $D = (3.81 \pm 0.36) \times 10^{-9}$ cm^2/s and $R = 43 \pm 2\%$. This mobile fraction is statistically the same as that of TrkA+gp75. The widths of the distributions for *R*'s are also not significantly different. The diffusion coefficent is significantly faster ($p \leq 0.0005$) and the distribution of *D*'s is significantly broader (*F*-test, $p \leq 0.01$). Addition of 4 nM NGF led to $D = (1.64 \pm 0.38) \times 10^{-9}$ cm^2/s and $R = 25 \pm 1\%$. Thus, NGF caused decreases in both the mobile fraction ($p \leq 0.0005$) and the diffusion coefficient *D* ($p \leq 0.0005$) and narrows both distributions (*F*-test, $p \leq 0.01$). This leads to the important conclusion that, in the presence of gp75, NGF-induced immobilization does not require a functional kinase domain or autophosphorylation of TrkA. The simplest explanation of this result is that NGF cross-links the NGF receptors to form immobile oligomers. This model will be discussed further below.

Diffusion of TrkA Expressed Alone. Use of the Sf9 cell system further enabled us to study the mobility of TrkA in the absence of gp75. It is known that NGF can activate TrkA in the absence of gp75 (*47*), resulting in signaling via two pathways: (1) phosphorylation of Y490 and activation of the SHC pathway and (2) phosphorylation of Y785 and activation of the PLCγ1 pathway (*40*, *48*).

We found for TrkA expressed in Sf9 cells $D = (2.64 \pm 0.21) \times 10^{-9}$ cm^2/s and $R = 46 \pm 2\%$. Addition of 4 nM NGF caused an approximate halving of the mobile fraction to $R = 23 \pm 1\%$ ($p \leq 0.0005$) and a slight reduction in the diffusion coefficient to $D = (1.73 \pm 0.11 \times 10^{-9}$ cm^2/s) (p ≤ 0.005). There also was a narrowing of both the distribution of *R* and *D* (*F*-test, $p \leq 0.01$). Thus, NGF-induced immobilization of TrkA on Sf9 cells does not require coexpression of gp75.

The effect of NGF on diffusion of TrkA was further investigated using mutated forms of TrkA. TrkA (K538N), which lacks phosphorylation activity, gave $D = (2.72 + 0.47 \times 10^{-9}$ cm^2/s) and $R = 34 \pm 1\%$. Addition of 4 nM NGF gave $D = (2.27 \pm 0.25 \times 10^{-9}$ cm^2/s) and $R = 36 \pm 1\%$. Thus, NGF had no significant effect on *R* for TrkA (K538N). NGF did not significantly alter the width of the distribution of *R*'s but did narrow the distribution of *D*'s (*F*-test, $p \leq 0.01$). In the absence of gp75, NGF-induced immobilization of TrkA requires an intact kinase domain.

Phosphorylation and Diffusion of TrkA in the Absence of gp75. We also note that the *R* for TrkA (K538N) was significantly lower (Student *t*-test, $p \leq 0.0005$) than that for wild-type TrkA and the distribution of *R*'s was significantly narrower (*F*-test, $p \leq 0.01$). Similar results were also obtained for two other mutants with reduced autophosphorylation (*16*, *17*). A mutant that lacks the three phosphorylation sites in the kinase regulatory domain of TrkA, TrkA(YYY/670,674,675/FFF) gave $D = (2.89 \pm 0.25 \times$

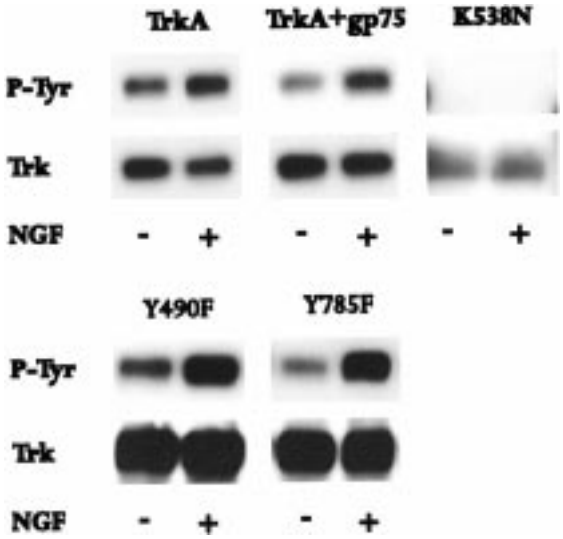

FIGURE 7: NGF-induced phosphorylation of TrkA. Sf9 cells treated with or without 4 nM NGF were extracted, and TrkA was immunoprecipitated. Tyrosine phosphorylation was assayed by Western blotting with anti-phosphotyrosine antibodies. The blots were stripped and then probed with anti-Trk antibodies to check the even loading of the gel. NGF-induced phosphorylation was observed for both TrkA and (gp75 + TrkA)-expressing cells. No phosphorylation was detected for TrkA (K538N), which bears a defective kinase domain.

10^{-9} cm^2/s) and $R = 32 \pm 1\%$ in the absence of NGF and $D = (2.62 \pm 0.24 \times 10^{-9}$ cm^2/s) and $R = 35 \pm 2\%$ in the presence of 4 nM NGF. A mutant lacking both the SHC and PLCγ1 sites TrkA(YY/490,785/FF) gave $D = (2.59 \pm 0.23 \times 10^{-9}$ cm^2/s) and $R = 30 \pm 1\%$ in the absence of NGF and $D = (3.04 \pm 0.39 \times 10^{-9}$ cm^2/s) and $R = 33 \pm 1\%$ in the presence of NGF. Thus, neither of these two mutants showed a significant NGF-induced immobilization based on the Student *t*-test. Results from these mutants further support the conclusion that NGF-induced immobilization of TrkA expressed by itself requires phosphorylation of at least one of the activation sites. These mutants such as TrkA (K538N) also showed reduced mobility compared to wild-type TrkA.

To further analyze the relationship between TrkA phosphorylation and lateral mobility, we determined the effects of NGF on phosphorylation of wild-type and mutated TrkA receptors. TrkA was immunoprecipitated from cell extracts, and phosphorylation on tyrosine residues was assessed by immunoblotting with anti-phosphotyrosine antibody (Figure 7). To detect small differences in the loading of the gel, the membrane was then stripped and reprobed with anti-Trk antibodies. Significantly, in the Sf9 system, there is some spontaneous autophosphorylation, probably resulting from the relatively high concentrations of these receptors. For our purposes, it represents an advantage of the Sf9 cell system since it enables us to separate the effects of phosphorylation from NGF-induced cross-linking. This spontaneous phosphorylation must be substoichiometric since one clearly observes, for both TrkA-expressing cells and (gp75+TrkA)-expressing cells, NGF enhancement of TrkA autophosphorylation. No tyrosine phosphorylation was detected for cells expressing TrkA (K538N), a mutation known to inactivate the kinase domain. Recognizing TrkA (K538N) as the unphosphorylated state of the receptor with $R = 34 \pm 1\%$, we conclude that spontaneous phosphorylation of wild-type TrkA leads to increased mobility $R = 43 \pm 1\%$ in the absence of NGF-induced cross-linking.

How is it that spontaneous phosphorylation leads to increased mobility even though it is at a substoichiometric level and NGF-induced phosphorylation leads to immobilization? An answer to this seeming paradox is suggested by mutants that lack one of the activation sites. Elimination of the SHC binding site TrkA (Y490F) showed $D = (1.95 \pm 0.14 \times 10^{-9}$ cm^2/s) and $R = 47 \pm 2\%$ in the absence of NGF and $D = (2.66 \pm 0.20 \times 10^{-9}$ cm^2/s) and $R = 48 \pm 2\%$ in the presence of 4 nM NGF. This suggests that phosphorylation of the PLCγ1 binding site is required for the increased mobility associated with spontaneous phosphorylation, but NGF-induced immobilization requires phosphorylation of the SHC binding site at Y490. This dichotomy is further supported by our results for TrkA (Y785F) where we observed $D = (2.03 \pm 0.16 \times 10^{-9}$ cm^2/s) and $R = 38 \pm 1\%$ in the absence of NGF and $D = (2.59 + 0.19 \times 10^{-9}$ cm^2/s) and $R = 33 \pm 1\%$ in the presence of NGF. NGF causes a small but statistically significant immobilization ($p \leq 0.005$). In the Discussion, we propose a model where phosphorylation of the PLCγ1 site activates protein kinase C and, thereby, increases mobility. The spontaneously dimerized TrkA receptors may be immobilized, but we have not detected this population, perhaps because of the mobilizing PKC effect and the small fraction of spontaneously activated TrkA molecules. At the same time, phosphorylation of Y490 causes the TrkA to interact with SHC protein in signaling complexes. This effectively increases the valency of the TrkA allowing NGF to cross-link it into immobile oligocomplexes.

DISCUSSION

We draw four basic conclusions from this study: (1) On PC12 cells, which are a common model for neuronal cells, both TrkA and gp75 are relatively immobilized. Such immobilization may provide a basis for functional regionalization of NGF receptors to neuronal domains or structures, such as synapses (*49*). (2) NGF causes further TrkA immobilization by a kinase-dependent mechanism. (3) This kinase-dependent immobilization requires the phosphorylation of specific tyrosines, such as the SHC binding site at Y490. (4) In contrast, TrkA in the presence of gp75 is immobilized by NGF in a kinase-independent manner.

To explain NGF-induced immobilization of TrkA, we propose a model based on current concepts of signal transduction (*34*). In this context, NGF cross-links two TrkA receptors, thereby activating the tyrosine kinase domains and inducing autophosphorylation (*50*). Phosphorylation of Y490 and Y785 results in binding of the SHC protein and PLCγ1 (*40, 48, 51, 52*). This signaling complex may then cross-link to additional proteins at the cytoplasmic face of the membrane, thereby, further reducing lateral diffusion. Immobilization might result from the increased size of the TrkA complex or from interactions of the cytoplasmic domain with the cytoskeleton. Each SHC molecule has a SH2 and a novel phosphotyrosine-binding domain (*53*) and, hence, might cross-link TrkA to other phosphotyrosine-bearing molecules. It also is intriguing that both SHC and PLCγ1 bind to the actin cytoskeleton (*54, 55*).

We consistently found that NGF-induced immobilization of TrkA expressed in Sf9 cells is coupled to a narrowing of

the distribution of mobile fractions (*F*-tests). One would expect such a phenomenon to result simply from the fact that *R* cannot be less than zero, so that the distribution becomes compressed as the mean *R* decreases. However, it is surprising that even for *R* distributions with low means there are very few zeros. This is despite the fact that the FRAP instrument is able to measure very low *R*'s. This may indicate a heterogeneity of receptors; i.e., there may be a small fraction of receptors (about 10%) that cannot be immobilized.

Analysis of TrkA receptors with mutated autophosphorylation sites is complex, but it is clear that the largest NGF-induced immobilization occurs with wild-type TrkA, suggesting that immobilization is a synergistic response to phosphorylation of multiple sites. A smaller, but significant, NGF-induced immobilization occurs for TrkA (Y785F), which has an intact SHC binding site but lacks the PLCγ1 binding site. These data suggest the SHC binding site may play a relatively important role in receptor immobilization.

In the absence of NGF, some of the mutated TrkA receptors, including the kinase-inactive TrkA (K538N) and TrkA (Y785F), are less mobile than wild-type TrkA. TrkA (Y490F), which has an intact PLCγ1 binding site, did not show this shift. It is possible that phosphorylation of other membrane proteins by TrkA or activation of PLCγ1 enhances lateral diffusion of membrane proteins. Since PLCγ1 activates protein kinase C (PKC), we tested whether phorbol ester, a potent activator of PKC, influenced TrkA mobility. In preliminary studies not shown, we found that phorbol ester increased the *R* for TrkA expressed in Sf9 cells. Further studies are now in progress to see if this is a general finding applicable to other cell types. Given these results, we propose that mobility of TrkA is determined by two opposing mechanisms. Spontaneous activation of a small fraction of TrkA molecules activates PLCγ1 and PKC, increasing *R*, while the addition of NGF results in dimerization, activation, and immobilization of a much larger fraction of TrkA molecules.

In the presence of gp75, NGF-induced immobilization of TrkA is independent of phosphorylation activity. We propose that, whereas NGF induces dimerization of TrkA, NGF induces formation of larger gp75-TrkA aggregates, which diffuse slowly, if at all. A possible simple mechanism is that gp75-TrkA binds NGF with a greater valency than TrkA does. Although it has been proposed that both receptors in the gp75-TrkA complex bind the same NGF molecule (*28*), there may be additional configurations. If the two receptors bound separate NGF molecules, then binding of NGF might result in polymerization or clustering of NGF receptors, e.g., (gp75-TrkA)−NGF−(TrkA-gp75)−NGF−(gp75-TrkA)−NGF−(TrkA-gp75). Alternatively, gp75 could induce a change in the TrkA conformation that allows more efficient oligomerization. A similar model has recently been suggested for T-cell receptors, in which binding of ligand leads to low-affinity lateral interactions between the CD3 and CD4 receptors, resulting in receptor clustering and signal transduction (*56*). Since TrkA and the T-cell receptor have quite different structures, the proposed model may describe multiple types of receptor proteins.

Interpretation and modeling of TrkA diffusion are ultimately dependent upon the nature and cause of immobile fractions in FRAP measurements, a currently active area of research. A variety of models for membrane diffusion have been proposed: free diffusion, free diffusion with obstacles, diffusion with sticky interacting obstacles, and corralled diffusion (*57*−*61*). Studies using the technique of single-particle tracking indicate that there are true immobile fractions which possibly result from anchoring or tethering of integral membrane proteins to the cytoskeleton while other immobile fractions result from corralling of membrane proteins into domains on the cell surface. Membrane proteins diffuse freely within the domain; their rate of movement over larger distances depends upon the rate of moving from one corral to the next. A monomer or dimer of TrkA might diffuse through the opening connecting one corral with the next, while a higher order aggregate might not (*61*). Recently Feder et al. (*60*) developed a unified theory of membrane diffusion which recognizes that as a protein diffuses along its local environment, its interactions with the environment changes. Such long tail kinetic models (*60*) result in recovery curves very similar to those predicted by the corral model (*61*). Until these issues are more clearly resolved, we must view the immobile fraction in a FRAP measurement as an empirical parameter which indicates the fraction of molecules that do not freely diffuse over the distance of about $\sim$1 μm in about 10 min; that is, they have an effective diffusion coefficient of $<10^{-12}$ cm^2/s.

Analysis of the shape and width of the distribution of *D* values may provide a clearer basis for distinguishing between models of the mobile fraction (*58, 59*). The heterogeneity which we observed in *D* on PC12 cells is similar to that observed by others in mammalian cells (*62*−*66*). The heterogeneity we observed on Sf9 cells is somewhat greater. Nevertheless, our data are largely confined to the region of $\sim 1 \times 10^{-9}$ to 5×10^{-9} cm^2/s. This range of $\sim$5-fold is larger than that predicted by free diffusion or diffusion with random obstacles (*58*). However, it is still much narrower than predicted by theoretical modeling of escape probabilities for a corral model (*59*). It falls within the range of *D* distributions predicted for various models that, like the long-tail kinetic model (*60*), allow for interaction of the diffusing molecule with randomly distributed obstacles (*59*). Thus, our results suggest that mobile TrkA receptors are not corralled by cytoskeletal elements and that heterogeneous diffusion results from specific interactions of TrkA receptors with other membrane components.

Ligand-induced immobilization of receptors occurs by two mechanisms. The first involves receptor autophosphorylation and interactions with signal transducing molecules such as SHC and PLPCγ1. The second is independent of autophosphorylation and may be due to receptor cross-linking and aggregation. Despite this advance in mechanistic understanding, we do not yet know the function of ligand-induced immobilization. We can propose two possibilities. The first is based on recent findings that some soluble kinases have associated subunits that bind to particular structures in the cell and, thereby, spatially restrict the kinase and the resulting phosphorylation (*67*). It may be that immobilization of receptor kinases places the receptor in the vicinity of certain membrane substrates critical for the biological response. For example, in some cases, NGF is released by an innervated target, diffuses across the synapse, and stimulates TrkA receptors on the neuron. Highly phosphorylated forms of TrkA, because they are immobile, might persist and signal

only at the synapse. Partially phosphorylated forms might diffuse, be internalized, be transported back to the neuronal cell body, and, thereby, signal at a different physical site. The second possibility is that diffusion of activated receptors might in some cases corrupt spatial information. NGF can act as a chemoattractant for neuronal growth cones (*68*). If the [NGF] were greater to the right of the growth cone than to the left, then more NGF−TrkA complexes would form on the right side of the growth cone than the left. The off-rate for NGF from the high-affinity NGF receptor is slow, and with a diffusion coefficent $\sim 10^{-9}$ cm^2/s mobile activated TrkA receptors would diffuse to the left side of the growth cone (~ 2 μm) in tens of seconds, that is, before NGF dissociates and TrkA is inactivated. Hence, diffusion of activated TrkA molecules would scramble spatial information. Immobilization of TrkA would enhance detection of NGF gradients. Further study using antibodies specific for phosphorylated segments of TrkA would be of interest to detect phosphorylation gradients or other localizations of different phosphorylated forms of TrkA (*69*).

REFERENCES

1. Levi, A., Shechter, Y., Neufeld, E. J., and Schlessinger, J. (1980) *Proc. Natl. Acad. Sci. U.S.A. 77*, 3469−3473.
2. Shechter, Y., Schlessinger, J., Jacobs, S., Chang, K. J., and Cuatrecasas, P. (1978) *Proc. Natl. Acad. Sci. USA 75*, 2135−2139.
3. Schlessinger, J., Shechter, Y., Willingham, M. C., and Pastan, I. (1978) *Proc. Natl. Acad. Sci. U.S.A. 75*, 2659−2663.
4. Snider, W. D. (1994) *Cell 77*, 627−638.
5. Barbacid, M. (1993) *Oncogene 8*, 2033−2042.
6. Chao, M. V. (1992) *Neuron 9*, 583−593.
7. Johnson, D., Lanahan, A., Buck, C. R., Sehgal, A., Morgan, C., Mercer, E., Bothwell, M., and Chao, M. (1986) *Cell 47*, 545−554.
8. Radeke, M. J., Misko, T. P., Hsu, C., Herzenberg, L. A., and Shooter, E. M. (1987) *Nature 325*, 593−597.
9. Volonte, C., Ross, A. H., and Greene, L. A. (1993) *Mol. Biol. Cell 4*, 71−78.
10. Canossa, M., Twiss, J. L., Verity, A. N., and Shooter, E. M. (1996) *EMBO J. 15*, 3369−3379.
11. Dobrowsky, R. T., Werner, M. H., Castellino, A. M., Chao, M. V., and Hannun, Y. (1994) *Science 265*, 1596−1599.
12. Wood, J. N. (1995) *Neurosci. Letts. 192*, 41−44.
13. Carter, B. D., Kaltschmidt, C., Kaltschmidt, B., Offenhauser, N., Bohm-Matthaei, R., Baeuerle, P. A., and Barde, Y.-A. (1996) *Science 272*, 542−545.
14. Grob, P. M., Ross, A. H., Koprowski, H., and Bothwell, M. (1985) *J. Biol. Chem. 260*, 8044−8049.
15. Taniuchi, M., Johnson, E. M., Roach, P. J., and Lawrence, J. C. (1986) *J. Biol. Chem. 261*, 13342−13349.
16. Guiton, M., Gunn-Moore, F. J., Stitt, T. N., Yancopoulos, G. D., and Tavare, J. M. (1994) *J. Biol. Chem. 269*, 30370−30377.
17. Cunningham, M. E., Stephens, R. M., Kaplan, D. R., and Greene, L. A. (1997) *J. Biol. Chem. 272*, 10957−10967.
18. Lee, K.-F., Li, E., Huber, J., Landis, S. C., Sharpe, A. H., Chao, M. V., and Jaenisch, R. (1992) *Cell 69*, 737−749.
19. Johnson, E. M., Taniuchi, M., Clark, H. B., Springer, J. E., Koh, S., Tayrien, M. W., and Loy, R. (1987) *J. Neurosci. 7*, 923−929.
20. Loy, R., Lachyankar, M. B., Condon, P. J., Poluha, D. K., and Ross, A. H. (1994) *Exp. Neurol. 130*, 377−386.
21. Ehlers, M. D., Kaplan, D. R., Price, D. L., and Koliatsos, V. E. (1995) *J. Cell Biol. 130*, 149−156.
22. Hempstead, B. L., Schleifer, L. S., and Chao, M. V. (1989) *Science 243*, 373−375.
23. Matsushima, H., and Bogenmann, E. (1990) *Mol. Cell. Biol. 10*, 5015−5020.
24. Pleasure, S. J., Reddy, U. R., Venkatakrishnan, G., Roy, A. K., Chen, J., Ross, A. H., Trojanowski, J. Q., Pleasure, D. E., and Lee, V. M. Y. (1990) *Proc. Natl. Acad. Sci. U.S.A. 87*, 8496−8500.
25. Verdi, J. M., Birren, S. J., Ibanez, C. F., Persson, H., Kaplan, D. R., Benedetti, M., Chao, M. V., and Anderson, D. J. (1994) *Neuron 12*, 733−745.
26. Hantzopoulos, P. A., Suri, C., Glass, D. J., Goldfarb, M. P., and Yancopoulos, G. D. (1994) *Neuron 13*, 187−201.
27. Jing, S., Tapley, P., and Barbacid, M. (1992) *Neuron 9*, 1067−1079.
28. Hempstead, B. L., Martin-Zanca, D., Kaplan, D. R., Parada, L. F., and Chao, M. V. (1991) *Nature 350*, 678−683.
29. Mahadeo, D., Kaplan, L., Chao, M. V., and Hempstead, B. L. (1994) *J. Biol. Chem. 269*, 6884−6891.
30. Chandler, C. E., Parsons, L. M., Hosang, M., and Shooter, E. M. (1984) *J. Biol. Chem. 259*, 6882−6889.
31. Barker, P. A., and Shooter, E. M. (1994) *Neuron 13*, 203−215.
32. Wolf, D. E., McKinnon, C. A., Daou, M.-C., Stephens, R. M., Kaplan, D. R., and Ross, A. H. (1995) *J. Biol. Chem. 270*, 2133−2138.
33. Ross, A. H., Daou, M.-C., McKinnon, C. A., Condon, P. J., Lachyankar, M. B., Stephens, R. M., Kaplan, D. R., and Wolf, D. E. (1996) *J. Cell Biol. 132*, 945−953.
34. Heldin, C.-H. (1995) *Cell 80*, 213−223.
35. Chapman, B. S., and Kuntz, I. D. (1995) *Protein Sci. 4*, 1696−1707.
36. Clary, D. O., Weskamp, G., Austin, L. R., and Reichardt, L. F. (1994) *Mol. Biol. Cell 5*, 549−563.
37. Venkatakrishnan, G., McKinnon, C. A., Ross, A. H., and Wolf, D. E. (1990) *Cell Regul. 1*, 605−614.
38. Venkatakrishnan, G., McKinnon, C. A., Pilapil, C. G., Wolf, D. E., and Ross, A. H. (1991) *Biochemistry 30*, 2748−2753.
39. Hempstead, B. L., Rabin, S. J., Kaplan, L., Reid, S., Parada, L. F., and Kaplan, D. R. (1992) *Neuron 9*, 883−896.
40. Stephens, R. M., Loeb, D. M., Copeland, T. D., Pawson, T., Greene, L. A., and Kaplan, D. R. (1994) *Neuron 12*, 691−705.
41. Matthews, J. A., Batki, A., Hynds, C., and Kricka, L. J. (1985) *Anal. Biochem. 151*, 205−209.
42. Stephani, U., Sutter, A., and Zimmerman, A. (1987) *J. Neurosci. Res. 17*, 25−35.
43. Wolf, D. E. (1989) *Methods Cell Biol. 30*, 271−306.
44. Axelrod, D., Koppel, D. E., Schlessinger, J., Elson, E., and Webb, W. W. (1976) *Biophys. J. 16*, 1055−1069.
45. Bevington, P. R. (1992) *Data reduction and error analysis for the physical sciences*, McGraw-Hill, New York.
46. Wolf, D. E., and Edidin, M. (1981) in *Techniques in Cellular Physiology* (Finean, J. B., and Michell, R. H., Eds.) pp 1−4, Elsevier/North Holland Biomedical Press, Amsterdam.
47. Klein, R., Jing, S., Nanduri, V., O'Rourke, E., and Barbacid, M. (1991) *Cell 65*, 189−197.
48. Obermeier, A., Bradshaw, R. A., Seedorf, K., Choidas, A., Schlessinger, J., and Ullrich, A. (1994) *EMBO J. 13*, 1585−1590.
49. Hafidi, A., Moore, T., and Sanes, D. H. (1996) *J. Comput. Neurol. 367*, 454−464.
50. Mohammadi, M., Schlessinger, J., and Hubbard, S. R. (1996) *Cells 86*, 577−587.
51. Greene, L. A., and Kaplan, D. R. (1995) *Curr. Biol. 5*, 579−587.
52. Obermeier, A., Halfter, H., Wiesmuller, K.-H., Jung, G., Schlessinger, J., and Ullrich, A. (1993) *EMBO J. 12*, 933−941.
53. van der Geer, P., and Pawson, T. (1995) *Trends Biochem. Sci. 20*, 277−280.
54. Thomas, D., Patterson, S. D., and Bradshaw, R. A. (1995) *J. Biol. Chem. 270*, 28924−28931.
55. Bar-Sagi, D., Rotin, D., Batzer, A., Mandiyan, V., and Schlessinger, J. (1993) *Cell 74*, 83−91.
56. Germain, R. N. (1997) *Curr. Biol. 7*, R640−R644.
57. Zhang, F., Lee, G. M., and Jacobson, K. (1993) *BioEssays 15*, 579−588.

58. Saxton, M. J. (1995) *Biophys. J. 69*, 389−398.
59. Saxton, M. J. (1997) *Biophys. J. 72*, 1744−1753.
60. Feder, T. J., Brust-Mascher, I., Slattery, J. P., Baird, B., and Webb, W. W. (1996) *Biophys. J. 70*, 2767−2773.
61. Kusumi, A., and Sako, Y. (1996) *Curr. Opin. Cell Biol. 8*, 566−574.
62. Livneh, E. R., Benveniste, M., Prywes, R., Felder, S., Kam, Z., and Schlessinger, J. (1986) *J. Cell Biol. 103*, 327−331.
63. Scullion, B. F., Hou, Y., Puddington, L., Rose, J. K., and Jacobson, K. (1987) *J. Cell Biol. 105*, 69−75.
64. Dragsten, P., Henkert, P., Blumenthal, R., Weinstein, J., and Schlessinger, J. (1979) *Proc. Natl. Acad. Sci. U.S.A. 76*, 5163−5167.
65. Edidin, M., and Wei, T. (1982) *J. Cell Biol. 95*, 458−462.
66. Wolf, D. E., Edidin, M., and Dragsten, P. R. (1980) *Proc. Natl. Acad. Sci. U.S.A. 77*, 2043−2045.
67. Faux, M. C., and Scott, J. D. (1996) *Trends Biochem. Sci. 21*, 312−315.
68. Gunderson, R. W., and Barrett, J. N. (1980) *J. Cell Biol. 87*, 546−554.
69. Segal, R. A., Bhattacharyya, A., Rua, L. A., Alberta, J. A., Stephens, R. M., Kaplan, D. R., and Stiles, C. D. (1996) *J. Biol. Chem. 271*, 20175−20181.

BI9719253